JACS
JOURNAL OF THE AMERICAN CHEMICAL SOCIETY

Communication

pubs.acs.org/JACS

Ultrahigh Nanoparticle Stability against Salt, pH, and Solvent with Retained Surface Accessibility via Depletion Stabilization

Xu Zhang,[†,‡] Mark R. Servos,[‡] and Juewen Liu*[,†]

[†]Department of Chemistry and Waterloo Institute for Nanotechnology and [‡]Department of Biology, University of Waterloo, 200 University Avenue West, Waterloo, Ontario, Canada N2L 3G1

Supporting Information

ABSTRACT: For many applications, it is desirable to stabilize colloids over a wide range of buffer conditions while still retaining surface accessibility for adsorption and reaction. Commonly used charge or steric stabilization cannot achieve this goal since the former is sensitive to salt and the latter blocks the particle surface. We use depletion stabilization in the presence of high molecular weight polyethylene glycol (PEG) to stabilize a diverse range of nanomaterials, including gold nanoparticles (from 10 to 100 nm), graphene oxide, quantum dots, silica nanoparticles, and liposomes in the presence of Mg^{2+} (>1.6 M), heavy metal ions, extreme pH (pH 1−13), organic solvents, and adsorbed nucleosides and drugs. At the same time, the particle surface remains accessible for adsorption of both small molecules and macromolecules. Based on this study, high loading of thiolated DNA was achieved in one step with just 2% PEG 20 000 in 2 h.

Stabilization of colloidal systems is one of the most important and fundamental aspects of nanoscience, enabling a diverse range of applications in physical and biological desciplines.[1] Charge stabilization is easy to achieve by means of electrostatic repulsion. For example, citrate-capped gold nanoparticles (AuNPs) are negatively charged and stable in <10 mM Na^+ for many years.[2] With a slight increase in salt concentration (e.g., >30 mM Na^+), aggregation starts to occur because of charge screening, and AuNPs can approach each other to experience London attractive force.[3,4] Therefore, charge stabilization is limited by several factors, including susceptibility to salt and the need for polar solvents. If a particle surface is coated with polymers, such as thiolated polyethylene glycol (PEG), and the size of the polymer is greater than the London interaction range, then steric stabilization might be achieved.[5] However, the coated polymers also block the particle surface from adsorbing other molecules. A combination of charge and steric stabilization is also possible, where AuNP capped by thiolated DNA is a good example.[6] For many applications involving nanoparticles, such as surface enhanced spectroscopy, nanoparticle bioconjugation, catalysis, heavy metal detection, and drug delivery, eliminating the colloidal stability problem while still retaining surface accessibility is highly desirable. Charge or steric stabilization, however, cannot achieve this goal.

When dispersed in a nonadsorbing polymer solution, nanoparticles may experience a depletion force originated from the excluded volume effect, for which no specific binding between the nanoparticle and polymer is required.[7] Theoretic calculations suggest both short-ranged depletion attraction and long-ranged depletion repulsion.[8] Depletion repulsion occurs when the nanoparticle separation is greater than the correlation length ξ of polymer concentration fluctuation in the bulk solution. In a semidilute polymer solution, ξ is much smaller than the size of the polymer.[9] Therefore, dispersed nanoparticles are repelled by each other unless they can approach to very close proximity, where the depletion force becomes attractive. More concentrated and higher molecular weight (MW) polymers produce stronger depletion forces.[10] Depletion stabilization has several advantages: First, colloidal stability might be less affected by ionic strength in comparison to charge stabilization. Second, in contrast to steric stabilization, nanoparticle surface should still be accessible since it is neither covalently modified nor strongly adsorbed by polymer.

Most experimental work on polymer depletion force was performed using concentrated silica or alumina particles to study their rheology properties.[11] Depletion force has found applications in nanoparticle purification,[12,13] self-assembly,[14] and protein crystallization.[15] However, important questions regarding salt-dependent colloidal stability as well as surface accessibility have not been systematically addressed. Herein, we explore AuNP stability in a diverse range of buffer conditions using PEG as the depletion agent, since PEG is chemically inert, cost-effective, and available with a wide range of MWs.[16] Compared to silica or alumina, the aggregation of AuNPs can be easily observed at a very low concentration (e.g., <0.02% w/w) via a red-to-blue color change (Figure 1).

We first tested the stability of citrate-capped 13 nm AuNPs in glycerol, ethylene glycol (EG), and PEG 200 and 400. The salt that came with the AuNPs was ∼10 mM Na^+, and no additional salt was added. AuNPs were stable even in 50% glycerol and EG as indicated by their characteristic red color (Figure 2A). However, purple aggregates were detected in >20% PEG 200 and 50% PEG 400. Since aggregation occurred only at high PEG concentrations, where the salt concentration remained low, and depletion force is proportional to PEG concentration, we reason that depletion attraction might be the main driving force for AuNP aggregation (Figure 1, green bars). Just three EG molecules polymerize into one PEG 200; the former is a small molecule, but the latter is a polymer and imparts the

Received: April 19, 2012
Published: May 30, 2012

   dx.doi.org/10.1021/ja303787e | J. Am. Chem. Soc. 2012, 134, 9910−9913

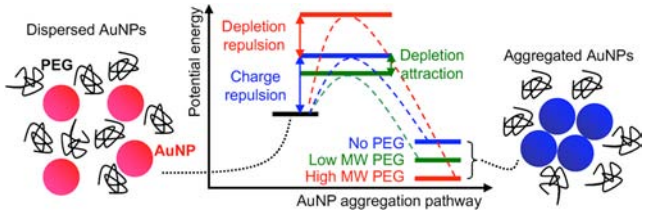

Figure 1. Schematics of the potential energy diagram of AuNP aggregation (not to scale). In the absence of PEG, AuNPs are stabilized by charge repulsion (blue bars). Low MW PEGs reduce the energy barrier for aggregation due to depletion attraction (green bars), while high MW PEGs increase the barrier height (red bars) due to depletion repulsion. Steric stabilization by adsorbed PEG is not considered in this diagram.

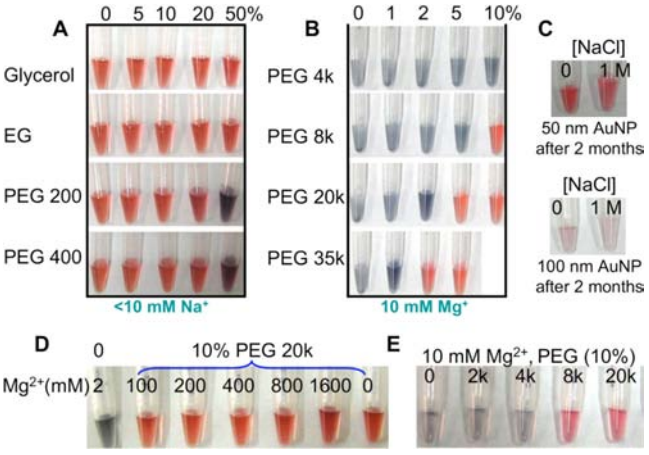

Figure 2. Stability of citrate-capped 13 nm AuNPs in the presence of various solutes. (A) Aggregation starts to occur in 20% (w/w) PEG 200 or 50% PEG 400 (no additional salt added). (B) Stability of AuNPs in 10 mM Mg^{2+}. Stabilization is achieved in high concentrations of high MW PEGs. (C) Long-term stabilization of AuNPs in 2% PEG 20000. AuNPs of (D) 13 nm and (E) 50 nm in the presence of various salt and PEG concentrations or molecular weights.

depletion effect.[17,18] Depletion repulsion appears insignificant for PEG 200 and 400 due to their low MW.[19]

Next we tested PEGs with MW greater 2000, where AuNPs remained stable in the absence of added salt (see SI). With 10 mM Mg^{2+}, stabilization was achieved with 10% PEG 8000, 5% PEG 20 000, or 2% PEG 35 000 (Figure 2B). Since charge repulsion was largely screened by Mg^{2+}, AuNP stability was attributed to depletion stabilization, although steric stabilization by adsorbed PEG cannot be ruled out at this moment. Consistent with theoretical calculations, our data also show that depletion stabilization is a function of PEG size; larger PEGs show the stabilization effective at lower concentrations. From the thermodynamic standpoint, PEG creates a crowded environment favorable for AuNP aggregation, and this is depicted in Figure 1 by the position of the red bar being the lowest after aggregation. To achieve aggregation, however, AuNPs need to overcome the depletion repulsion barrier on top of the electrostatic barrier. Even after screening the electrostatic barrier, the remaining depletion barrier can still be high enough to maintain colloidal stability.

To test the limit of salt that AuNPs can tolerate, we incubated 13 nm AuNPs in 10% PEG 20 000 with increasing concentration of Mg^{2+} (Figure 2D), where AuNPs remained stable even with 1.6 M $MgCl_2$. In contrast, 2 mM Mg^{2+} induced aggregation instantaneously in the absence of PEG. Without any covalent ligands, this level of stabilization against salt is quite remarkable. Next we tested larger AuNPs, which are known to be more difficult to stabilize.[20] We challenged 50 nm AuNPs dispersed in 10% PEGs with 10 mM Mg^{2+} (Figure 2E). Stabilization was achieved with PEG 8000 and higher, similar to the case of 13 nm AuNPs. We also tested long-term stability; 50 and 100 nm AuNPs remained stable even after incubating with 1 M NaCl in just 2% PEG 20 000 for 2 months at room temperature (Figure 2C).

AuNPs have been a popular probe for detecting heavy metal ions, which may also cause nonspecific AuNP aggregation.[21] We next studied the protection effect of PEG in the presence of 2−10 mM heavy metal ions (Figure 3A); AuNPs aggregated in

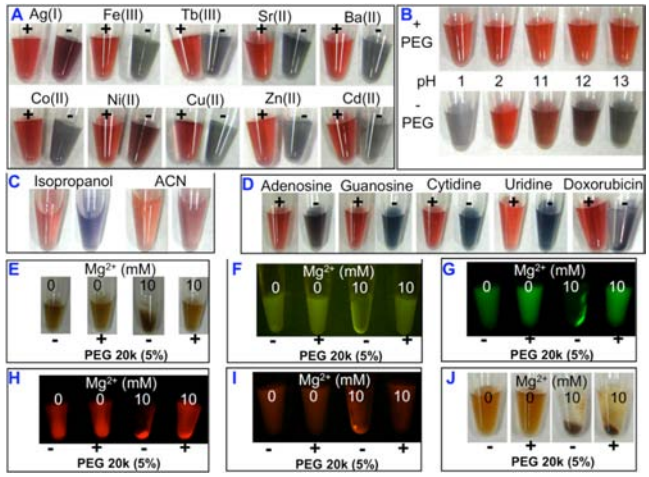

Figure 3. Effect of 2% PEG 20 000 on the stability of citrate-capped 13 nm AuNPs in the presence of (A) various heavy metal ions: 4 mM Ba^{2+}, 10 mM Sr^{2+}, and 2 mM for the rest; (B) buffer pH; (C) 67% organic solvents; and (D) ribonucleosides (A = 5 μM, G = 0.25 mM, C = 2 mM, U = 20 mM) and doxorubicin (2 μg/mL). (E) Stability of graphene oxide; (F) fluorescein-labeled 50 nm silica nanoparticles; (G) green quantum dots with surface carboxyl; (H) red quantum dots with surface hydroxyl; (I) rhodamine-labeled DOPG liposomes; and (J) iron oxide nanoparticles with surface organic amine in the presence or absence of PEG or Mg^{2+}. The "+" and "−" signs denote for the presence and absence of PEG.

water but 2% PEG 20 000 showed effective protection. The same PEG concentration was also able to protect AuNPs from pH 1 to 13 (Figure 3B) and in 67% isopropanol or acetonitrile (Figure 4C). Various nucleosides and doxorubicin can adsorb onto AuNPs and cause aggregation, which was also suppressed by PEG (Figure 4D). This may enable surface enhanced spectroscopy under a diverse range of conditions. We further tested other nanomaterials, including graphene oxide (Figure 4E), fluorescein-labeled 50 nm silica nanoparticles (Figure 4F), green and red fluorescent quantum dots (Figure 4G,H, respectively), rhodamine-labeled liposomes (Figure 4I) and iron oxide magnetic nanoparticles (Figure 4J). For all the materials, 10 mM Mg^{2+} induced aggregation in the absence of PEG. With 5% PEG 20 000, stabilization was achieved in most cases except for the magnetic nanoparticles, whose surface contained organic amine. It is likely that this surface ligand influenced the depletion force. The effect of nanoparticle surface property will be a subject of further studies. In general, high stability against salt in PEG is true for a diverse range of nanoparticle types and sizes.

dx.doi.org/10.1021/ja303787e | J. Am. Chem. Soc. 2012, 134, 9910−9913

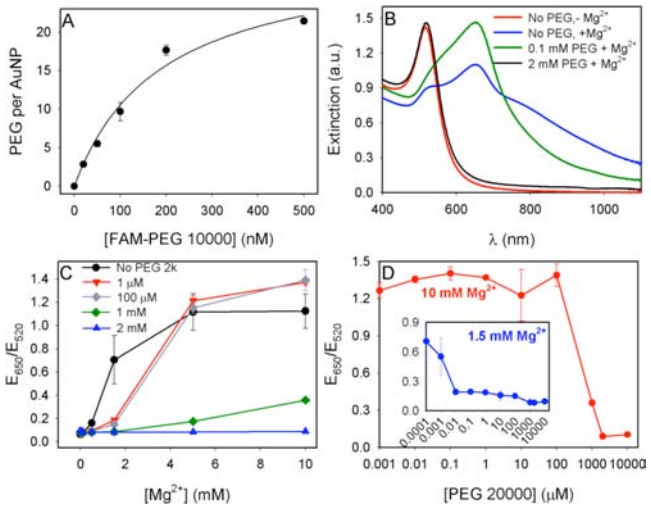

Figure 4. (A) Adsorption isotherm of FAM-labeled PEG 10 000 onto 5 nM 13 nm AuNPs. (B) UV−vis spectra of AuNPs in several PEG 20 000 concentrations in the presence or absence of 10 mM Mg^{2+}. (C) AuNP extinction ratio as a function of Mg^{2+} concentration in various concentrations of PEG 20 000. (D) The extinction ratio as a function of PEG 20 000 concentration in the presence of 10 and 1.5 mM Mg^{2+} (inset).

Although PEG is generally considered to be a nonadsorbing polymer, it has been reported that PEG can adsorb onto gold electrodes and similar materials.[22] Therefore, PEG might also be adsorbed by AuNPs and impart steric stabilization. To test whether the observed AuNP stabilization was indeed due to the depletion effect, the adsorption isotherm of a 6-carboxyfluorescein (FAM)-labeled PEG 10 000 was measured. AuNPs were mixed with various concentrations of the FAM-PEG, and the adsorbed PEG was quantified by measuring fluorescence quenching (Figure 4A). Indeed, a Langmuir adsorption isotherm was obtained, indicating monolayer and reversible PEG adsorption by AuNPs. With ∼500 nM PEG 10 000, the surface of AuNPs (5 nM) was saturated. The fact that even 1% PEG 20 000 (500 μM) failed to protect AuNPs (Figure 2B) strongly indicated the importance of PEG concentration beyond the monolayer coverage on AuNP surface.

To dissect the effect of depletion stabilization from steric stabilization, we performed a quantitative study using UV−vis spectroscopy. Dispersed AuNPs show a strong extinction peak at 520 nm due to surface plasmon (Figure 4B, red curve). In the absence of PEG, AuNPs immediately aggregated upon addition of 10 mM Mg^{2+} with the plasmon peak broadening and shifting to ∼650 nm (blue curve). In the presence of 0.1 mM PEG 20 000 (0.5%), AuNPs were still aggregated by Mg^{2+} (green curve), but 2 mM PEG 20 000 (4%) effectively stabilized the AuNPs (black curve). Using the ratio of extinction at 650 nm over 520 nm, we can quantify the aggregation state of AuNPs, and a higher ratio indicates aggregated AuNPs. AuNPs were dispersed in various concentrations of PEG, and Mg^{2+} was titrated to each sample (Figure 4C). Low concentrations of PEG have a moderate protection effect when Mg^{2+} concentration is below 1.5 mM, where samples containing PEG have extinction ratios <0.2, while the samples without PEG are ∼0.6. This is attributed to steric stabilization by the adsorbed PEG. This steric protection starts when the PEG concentration is greater than 10-100 nM (inset of Figure 5D), which is consistent with the PEG adsorption isotherm in Figure 4A. With a high Mg^{2+} concentration of 10 mM, steric stabilization is insufficient, and AuNPs aggregate even in the presence of 100 μM PEG 20 000 (Figure 4D). Depletion stabilization starts to take place with a PEG concentration of 1 mM (i.e., 2%), and highly effective stabilization is achieved at 2 mM. PEG 20 000 reaches the semidilute region at ∼5.1%,[23] where the PEG chains start to overlap. The onset of effective PEG protection is also around this concentration, further confirming the depletion stabilization mechanism. Taken together, steric protection by adsorbed PEG is effective only at low Mg^{2+} concentrations (e.g., <1.5 mM). For this reason, we did not consider steric stabilization in Figure 1.

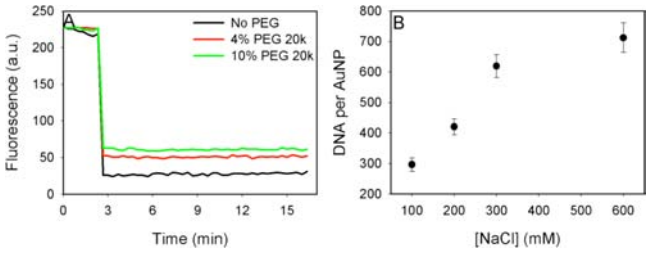

Figure 5. (A) Kinetics of doxorubicin fluorescence change upon mixing with AuNPs (at the 2.8 min time point) in the presence of varying concentrations of PEG 20 000. (B) Loading of thiolated DNA onto 50 nm AuNPs in 2% PEG 20 000 as a function of NaCl concentration.

So far we have demonstrated that high MW PEGs are effective for stabilizing various nanoparticles in a diverse range of buffer conditions, solving the salt sensitivity problem. The nanoparticle surface should remain accessible since the PEGs are only weakly and reversibly adsorbed. To test this, we mixed positively charged and fluorescent doxorubicin with AuNPs and monitored the kinetics of fluorescence change (Figure 5A). Without PEG, a quick drop in fluorescence was observed since AuNPs quenched adsorbed doxorubicin (black curve). The kinetics of adsorption in the presence of 4% and 10% PEG 20 000 were also very fast and finished within the first 20 s after mixing. Therefore, adsorption of small molecules was not impeded by PEG.

The unique properties of depletion stabilization allow us to carry out reactions that are difficult to achieve otherwise. For example, to attach a high density of thiolated DNA to AuNPs, a high salt concentration is required to screen the electrostatic repulsion between DNA and AuNPs.[24] Confined by the colloidal stability of AuNPs, however, this reaction cannot be performed directly in a high salt buffer, where AuNPs would aggregate before DNA adsorption takes place. To solve this problem, salt aging (i.e., gradually adding NaCl over 1−2 days) is the current standard protocol.[25] Surfactants need to be added to functionalize large AuNPs (e.g., 50 nm), and the slow salt aging is still required.[20] Using a fluorinated surfactant, DNA attachment can be finished in 2 h.[26] However, surfactants might be toxic to cells. We recently developed a low pH DNA-loading strategy that also allows for fast DNA attachment.[27] Our observations in this work provide an alternative method since a high concentration of salt can be added all at once without using surfactants. Kinetic experiments with a FAM-labeled thiolated DNA in 2% PEG 20 000 showed a biphasic trend with an initial fast adsorption followed by a slow phase. A higher salt concentration produced faster adsorption in both phases (see SI). Therefore, the AuNP surface is also accessible for the adsorption of macromolecules. After dispersing 50 nm AuNPs

in 2% PEG 20 000, we added the thiolated DNA in the presence of various concentrations of NaCl. After 2 h incubation, the attached DNA was quantified. As shown in Figure 5B, more DNAs were attached in higher NaCl concentrations. With 600 mM NaCl, we were able to load 719 ± 59 DNAs on each 50 nm AuNP in 2 h, comparable with that achieved using surfactants and salt aging over 1−2 days.[20,28]

In summary, we have shown that depletion force can be applied to achieve ultrahigh colloidal stability in extremely high ionic strength, extreme pH, organic solvents, heavy metals, and small molecule adsorbates, while still retaining surface accessibility. For most applications, just 2% PEG 20 000 is sufficient, and the viscosity brought by the polymer is very low. Depletion stabilization eliminates the disadvantages of charge or steric stabilization, enabling the exploration of many colloidal properties and reactions under otherwise forbiddingly high salt conditions. For example, we have demonstrated the quick loading of thiolated DNA onto AuNPs. Recently, various nanomaterials have been tested for drug delivery, disease diagnosis, and imaging applications.[1,29] When delivered into cells, these nanomaterials experience a crowded environment similar to the one reported in this work. The stability and interaction of nanoparticles with biomolecules are likely to be different from that in buffers. Therefore the depletion effect needs to be taken into consideration for the design of such materials. Finally, we demonstrated that AuNPs are useful for studying depletion force because of its extremely high extinction coefficients and distance-dependent color. Useful information can be obtained by a simple visual inspection.

■ ASSOCIATED CONTENT

Supporting Information

Materials and methods, TEM, AuNP stability, and DNA adsorption kinetics. This material is available free of charge via the Internet at http://pubs.acs.org.

■ AUTHOR INFORMATION

Corresponding Author

liujw@uwaterloo.ca

Notes

The authors declare no competing financial interest.

■ ACKNOWLEDGMENTS

Funding for this work is from the University of Waterloo, Canadian Foundation for Innovation, Early Researcher Award from Ontario Ministry of Research & Innovation, Canadian Institutes of Health Research, and the Natural Sciences and Engineering Research Council (NSERC) of Canada.

■ REFERENCES

(1) (a) Rosi, N. L.; Mirkin, C. A. *Chem. Rev.* **2005**, *105*, 1547−1562. (b) Alivisatos, A. P.; Gu, W.; Larabell, C. *Annu. Rev. Biomed. Eng.* **2005**, *7*, 55−76. (c) Daniel, M.-C.; Astruc, D. *Chem. Rev.* **2004**, *104*, 293−346. (d) Saha, K.; Agasti, S. S.; Kim, C.; Li, X.; Rotello, V. M. *Chem. Rev.* **2012**, 2739−2779. (e) Katz, E.; Willner, I. *Angew. Chem., Int. Ed.* **2004**, *43*, 6042−6108. (f) Wang, H.; Yang, R. H.; Yang, L.; Tan, W. H. *ACS Nano* **2009**, *3*, 2451−2460. (g) Zhao, W.; Brook, M. A.; Li, Y. *Chembiochem* **2008**, *9*, 2363−2371. (h) Li, D.; Song, S. P.; Fan, C. H. *Acc. Chem. Res.* **2010**, *43*, 631−641.

(2) Turkevich, J. *Gold Bulletin* **1985**, *18*, 86−91.

(3) London, F. *Z. Phys.* **1930**, *63*, 245−279.

(4) Enustun, B. V.; Turkevich, J. *J. Am. Chem. Soc.* **1963**, *85*, 3317−3328.

(5) (a) Wuelfing, W. P.; Gross, S. M.; Miles, D. T.; Murray, R. W. *J. Am. Chem. Soc.* **1998**, *120*, 12696−12697. (b) Zheng, M.; Davidson, F.; Huang, X. *J. Am. Chem. Soc.* **2003**, *125*, 7790−7791. (c) Latham, A. H.; Williams, M. E. *Langmuir* **2006**, *22*, 4319−4326.

(6) Mirkin, C. A.; Letsinger, R. L.; Mucic, R. C.; Storhoff, J. J. *Nature* **1996**, *382*, 607−609.

(7) Asakura, S.; Oosawa, F. *J. Polym. Sci.* **1958**, *33*, 183−192.

(8) (a) Asakura, S.; Oosawa, F. *J. Chem. Phys.* **1954**, *22*, 1255−1256. (b) Vrij, A. *Pure Appl. Chem.* **1976**, *48*, 471−483. (c) Mao, Y.; Cates, M. E.; Lekkerkerker, H. N. W. *Physica A* **1995**, *222*, 10−24.

(9) Semenov, A. N. *Macromolecules* **2008**, *41*, 2243−2249.

(10) Lekkerkerker, H. N. W.; Tuinier, R. *Colloids and the Depletion Interaction*; Springer: New York, 2011.

(11) (a) Ogden, A. L.; Lewis, J. A. *Langmuir* **1996**, *12*, 3413−3424. (b) Bakandritsos, A.; Psarras, G. C.; Boukos, N. *Langmuir* **2008**, *24*, 11489−11496. (c) Kim, S. Y.; Zukoski, C. F. *Langmuir* **2011**, *27*, 10455−10463.

(12) Park, K.; Koerner, H.; Vaia, R. A. *Nano Lett.* **2010**, *10*, 1433−1439.

(13) Khripin, C. Y.; Arnold-Medabalimi, N.; Zheng, M. *Acs Nano* **2011**, *5*, 8258−66.

(14) (a) Dinsmore, A. D.; Yodh, A. G.; Pine, D. J. *Nature* **1996**, *383*, 239−242. (b) Sacanna, S.; Irvine, W. T. M.; Chaikin, P. M.; Pine, D. J. *Nature* **2010**, *464*, 575−578. (c) Tam, J. M.; Murthy, A. K.; Ingram, D. R.; Nguyen, R.; Sokolov, K. V.; Johnston, K. P. *Langmuir* **2010**, *26*, 8988−8999. (d) Zhang, F.; Dressen, D.; Skoda, M.; Jacobs, R.; Zorn, S.; Martin, R.; Martin, C.; Clark, G.; Schreiber, F. *Eur. Biophys. J.* **2008**, *37*, 551−561.

(15) Tanaka, S.; Ataka, M. *J. Chem. Phys.* **2002**, *117*, 3504−3510.

(16) Miyoshi, D.; Sugimoto, N. *Biochimie* **2008**, *90*, 1040−1051.

(17) Pramanik, S.; Nakamura, K.; Usui, K.; Nakano, S.-i.; Saxena, S.; Matsui, J.; Miyoshi, D.; Sugimoto, N. *Chem. Commun.* **2011**, *47*, 2790−2792.

(18) Zaki, A.; Dave, N.; Liu, J. *J. Am. Chem. Soc.* **2012**, *134*, 35−38.

(19) (a) Burns, J. L.; Yan, Y.-d.; Jameson, G. J.; Biggs, S. *J. Colloid Interface Sci.* **2002**, *247*, 24−32. (b) Biggs, S.; Burns, J. L.; Yan, Y.-d.; Jameson, G. J.; Jenkins, P. *Langmuir* **2000**, *16*, 9242−9248. (c) Milling, A. J.; Kendall, K. *Langmuir* **2000**, *16*, 5106−5115. (d) Kuhl, T. L.; Berman, A. D.; Hui, S. W.; Israelachvili, J. N. *Macromolecules* **1998**, *31*, 8258−8263.

(20) Hurst, S. J.; Lytton-Jean, A. K. R.; Mirkin, C. A. *Anal. Chem.* **2006**, *78*, 8313−8318.

(21) (a) Kim, Y.; Johnson, R. C.; Hupp, J. T. *Nano Lett.* **2001**, *1*, 165−167. (b) Lin, Y.-W.; Huang, C.-C.; Chang, H.-T. *Analyst* **2010**, *136*, 863−871.

(22) (a) Mendez, A.; Moron, L. E.; Ortiz-Frade, L.; Meas, Y.; Ortega-Borges, R.; Trejo, G. *J. Electrochem. Soc.* **2011**, *158*, F45−F51. (b) Lee, P. C.; Meisel, D. *Chem. Phys. Lett.* **1983**, *99*, 262−265. (c) Napper, D. H.; Netschey, A. *J. Colloid Interf. Sci.* **1971**, *37*, 528−535. (d) Lin, S.; Cheng, Y.; Liu, J.; Wiesner, M. R. *Langmuir* **2012**, *28*, 4178−4186.

(23) Ziebacz, N.; Wieczorek, S. A.; Kalwarczyk, T.; Fialkowski, M.; Holyst, R. *Soft Matter* **2011**, *7*.

(24) (a) Elghanian, R.; Storhoff, J. J.; Mucic, R. C.; Letsinger, R. L.; Mirkin, C. A. *Science* **1997**, *277*, 1078−1080. (b) Herne, T. M.; Tarlov, M. J. *J. Am. Chem. Soc.* **1997**, *119*, 8916−8920. (c) Zhang, X.; Servos, M. R.; Liu, J. *Langmuir* **2012**, *28*, 3896−3902.

(25) Storhoff, J. J.; Elghanian, R.; Mucic, R. C.; Mirkin, C. A.; Letsinger, R. L. *J. Am. Chem. Soc.* **1998**, *120*, 1959−1964.

(26) Zu, Y.; Gao, Z. *Anal. Chem.* **2009**, *81*, 8523−8528.

(27) Zhang, X.; Servos, M. R.; Liu, J. *J. Am. Chem. Soc.* **2012**, *134*, 7266−7269.

(28) Hill, H. D.; Millstone, J. E.; Banholzer, M. J.; Mirkin, C. A. *ACS Nano* **2009**, *3*, 418−424.

(29) (a) Liu, J.; Cao, Z.; Lu, Y. *Chem. Rev.* **2009**, *109*, 1948−1998. (b) Rosi, N. L.; Giljohann, D. A.; Thaxton, C. S.; Lytton-Jean, A. K. R.; Han, M. S.; Mirkin, C. A. *Science* **2006**, *312*, 1027−1030.